Preparation and Characterization of Multiwalled Carbon Nanotube-Supported Platinum for Cathode Catalysts of Direct Methanol Fuel Cells

Wenzhen Li,[†] Changhai Liang,[‡] Weijiang Zhou,[†] Jieshan Qiu,[§] Zhenhua Zhou,[†] Gongquan Sun,[†] and Qin Xin*[,‡]

Direct Methanol Fuel Cell Laboratory and State Key Laboratory of Catalysis, Dalian Institute of Chemical Physics, Chinese Academy of Sciences, Dalian 116023, China, and Carbon Research Laboratory, Department of Materials Science and Chemical Engineering, Dalian University of Technology, Dalian 116012, China

Received: November 27, 2002; In Final Form: February 21, 2003

Multiwalled carbon nanotube-supported Pt (Pt/MWNT) nanocomposites were prepared by both the aqueous solution reduction of a Pt salt (HCHO reduction) and the reduction of a Pt ion salt in ethylene glycol solution. For comparison, a Pt/XC-72 nanocomposite was also prepared by the EG method. The Pt/MWNT catalyst prepared by the EG method has a high and homogeneous dispersion of spherical Pt metal particles with a narrow particle-size distribution. TEM images show that the Pt particle size is in the range of 2−5 nm with a peak at 2.6 nm, which is consistent with 2.5 nm obtained from the XRD broadening calculation. Surface chemical modifications of MWNTs and water content in EG solvent are found to be the key factors in depositing Pt particles on MWNTs. In the case of the direct methanol fuel cell (DMFC) test, the Pt/MWNT catalyst prepared by EG reduction is slightly superior to the catalyst prepared by aqueous reduction and displays significantly higher performance than the Pt/XC-72 catalyst. These differences in catalytic performance between the MWNT-supported or the carbon black XC-72-supported catalysts are attributed to a greater dispersion of the supported Pt particles when the EG method is used, in contrast to aqueous HCHO reduction and to possible unique structural and higher electrical properties when contrasting MWNTs to carbon black XC-72 as a support.

Introduction

Direct methanol fuel cells (DMFCs), a kind of polymer electrolyte fuel cell (PEFC), are attracting much more attention for their potential as clean and mobile power sources in the future.[1−6] However, there is a serious problem with DMFCs: the thermodynamic potential for DMFC is 1.19 V, which is only 40 mV less than that for PEFCs, but the overpotential at the cathode is about 0.3 V even under open-circuit conditions because of the high degree of irreversibility of the oxygen reduction reaction (ORR, 0.2 V loss); short circuits in the cathode reaction resulted from methanol crossover (0.1 V loss), which means a loss of about 25% from the theoretical maximum efficiency only in the cathode of a DMFC.[7] So far, some attempts have been made to find methanol-resistant cathode catalysts in DMFCs.[8−10] It has been found that carbon-supported binary and ternary alloys of platinum, namely, Pt−Co/C, Pt−Cr/C, and Pt−Cr−Co/C, show good performance in ORRs in PEFCs[11−13] and more recently in DMFCs.[7,14,15] It is well known that the specific activity of platinum metal in ORRs is also related to the carbon support.[16] The ideal support material should have the following characteristics: provide a high electrical conductivity, allow the reactant gas to get to the electrocatalyst easily, have adequate water-handling capability at the cathode where water is generated, and also show good corrosion resistance because cathodes in DMFCs are under strongly oxidizing conditions. Generally, the electrocatalysts are supported on high-surface-area carbon black with a high mesoporous distribution and graphite character, and in this case, XC-72 carbon black is the most widely used carbon support for the preparation of fuel cell catalysts because of its good compromise between electronic conductivity and the BET surface area.[4,17] To enhance the activity of ORRs, one strategy is to explore highly active catalysts with novel carbon material as a support. Carbon nanotubes (CNTs) have attracted much interest from both a fundamental and an applied perspective since their discovery[18] and large-scale synthesis,[19,20] owing to their good mechanical and unique electrical properties. These CNTs materials are also considered to be potentially useful supports in heterogeneous catalysis.[21−26] Nanoparticle Pt deposited on carbon tubule membranes[27] and highly ordered nanoporous arrays of carbon[28] synthesized by template synthesis methods have been shown to have superior electric activity in ORRs in a half-cell configuration. Graphite nanofiber (GNF) has also been considered to be a potential support for electrocatalysts, and it has been reported in a cyclic voltammetry study[29] that the GNF-supported electrocatalysts of platinum particles have high activities for the electrochemical oxidation of methanol. Recently, Lukehart's group[30−32] also prepared a Pt−Ru/herringbone GNF nanocomposite using a single-source molecular precursor as the metal source, and the performance of the DMFC with this nanocomposite as the anode catalyst was enhanced by 50% relative to that recorded by an unsupported Pt−Ru colloid anode catalyst. These studies strongly imply the possible

* To whom correspondence should be addressed. E-mail: xinqin@dicp.ac.cn. Tel: +86-411-4379071. Fax: +86-411-4379071.
[†] Direct Methanol Fuel Cell Laboratory, Dalian Institute of Chemical Physics.
[‡] State Key Laboratory of Catalysis, Dalian Institute of Chemical Physics.
[§] Dalian University of Technology.

10.1021/jp022505c CCC: $25.00
Published on Web 06/06/2003

application of novel carbon materials as catalyst supports in the electrodes of fuel cells.

Previously, we found that multiwalled carbon nanotube (MWNT)-supported platinum nanoparticles for cathode catalysts were found to have enhanced activity in the ORR in a DMFC.[33] In this paper, we reported two synthesis methods to prepare MWNT-supported platinum: one is an aqueous solution reduction of a Pt salt (HCHO reduction method), and the other is the reduction of the Pt ion salt in ethylene glycol solution (EG method). The influences of detailed preparation conditions of the EG method, such as surface chemical modification of MWNTs and water content in EG solvent, were investigated. XRD, TEM, and HRTEM characterizations were carried out to determine the particle size and distribution of the catalysts. These Pt-based catalysts were also employed as cathode catalysts in DMFC to investigate their ORR activity and single-cell performance.

Experimental Section

MWNTs used in this work were produced from high-purity graphite in a classical arc-discharge evaporation method.[18] The MWNTs mostly ranging from 4 to 60 nm in diameter are hollow tubular structures with a highly graphite multilayer wall.

The MWNTs in these experiments were purified by ultrasonic treatment for 10 min (Shanghai-Branson SB2200T, 50 kHz, 80 W) and then refluxed in 70% HNO_3 at 120 °C for 4 h. Surface oxidation of the MWNTs was accomplished with a 4.0 N $H_2SO_4-HNO_3$ mixture for 4 h under refluxing conditions, following a procedure reported in ref 26. After the oxidation treatment, a surface-oxidized MWNT sample was obtained with a yield of ca. 80 wt %. XC-72 carbon (Cabot Corp., Vulcan XC-72, BET surface area 237 m^2/g) was purified and oxidized by following a procedure reported in ref 34. The BET surface area of purified MWNTs with and without oxidization was determined by N_2 physisorption at 77 K using a Nova 4000 instrument (Quantachrome Corp.).

Pt-based catalysts were prepared by two methods. The first method was an HCHO reduction method in which 500 mg of surface-oxidized MWNTs prepared as described above was suspended in 50 mL of deionized (DI) water and stirred first with ultrasonic treatment for 20 min and then mechanically stirred for 4 h, during which time 7.5 mL of hexachloroplatinic acid with a concentration of 7.4 mg Pt/mL was added to the solution dropwise and 2.5 M NaOH was added to adjust the pH of solution to about 11. Formaldehyde (37%, 0.75 mL) was added to the solution to reduce Pt at 85 °C for 1.5 h, and a flow of argon was passed through the reaction system to isolate oxygen and to remove organic byproducts. The solid was filtered and washed with 1.5 L of DI water and then dried at 70 °C for 8 h. The Pt/MWNT (A) catalyst with a metal loading of 10 wt % was obtained. In the case of the EG method,[35,36] 500 mg of surface-oxidized MWNTs was suspended in 50 mL of ethylene glycol solution and stirred with ultrasonic treatment for 20 min; 7.5 mL of hexachloroplatinic acid EG solution (7.4 mg Pt/mL EG) was added to the solution dropwise also under mechanically stirred conditions for 4 h. NaOH (2.5 M in EG solution) was added to adjust the pH of the solution to above 13, and then the solution was heated at 140 °C for 3 h to ensure that Pt was completely reduced; the entire EG solution has a DI water content of 5 vol %. Refluxing conditions were used to keep water in the synthesis system. The whole preparation process was also conducted under flowing argon. Filtration, washing, and drying procedures are the same as for the HCHO method as described above. In this way, the final Pt/MWNT (B) catalyst sample with the same metal loading (10 wt %) was also obtained. For comparison, treated XC-72 carbon was also used as a support to prepare Pt/XC-72 catalysts with the same metal loading according to exactly the EG method procedures described above.

All of the Pt-based catalyst samples were characterized by recording their X-ray diffraction (XRD) patterns on a Rigaku Rotalflex (RU-200B) X-ray diffractometer using Cu Kα radiation with a Ni filter. The tube current was 100 mA with a tube voltage of 40 kV. The 2θ angular regions between 20 and 85° were explored at a scan rate of 5°/min. The Pt (220) peak (64−72°) was scanned at 1°/min to obtain the Pt particle size by using the Scherrer formula. For all XRD tests, the resolution in the 2θ scans was kept at 0.02°. TEM and HRTEM investigations were carried out in a JEOL JEM-2000EX operating at 100 keV and a JEOL JEM-2011 operating at 200 keV. The size distribution and the mean size of the Pt particles of the catalysts were obtained by measuring more than 200 particles from bright-field micrographs recorded on JEOL JEM-2000EX TEM images.

The electrochemical activity of the three Pt-based catalysts as cathode catalysts (metal loading 1.0 mg/cm^2) in DMFC was examined. The anode catalysts were Pt−Ru/C (Johnson Matthey Corp., 20 wt % Pt, 10 wt % Ru) with Nafion-115 (Dupont) as the membrane. The electrodes were prepared according to the following procedure: Both the anode and cathode consisted of a backing layer, a gas-diffusion layer, and a catalyst layer. Teflon-containing (30 wt % Teflon in cathode, 10 wt % Teflon in anode) carbon papers (SGL Corp., 270-μm thickness) were employed as backing layers in these electrodes. Teflon (10 or 30 wt %) in carbon black XC-72 was suspended in ethanol and agitated in an ultrasonic water bath, and then the slurry was spread onto the carbon paper as gas-diffusion layers (ca. 30-μm thickness). The required amount of catalyst (Pt−Ru/C in anode, 2.0 mg/cm^2 metal loading; Pt-based catalyst in cathode, in-house, 10 wt %, 1.0 mg/cm^2 metal loading) was mixed with 10 wt % Nafion (5 wt % Nafion solution) to constitute catalyst layers. Finally, a thin layer of 5 wt % Nafion solution was spread onto the surface of each electrode (1.0 mg Nafion/cm^2). Membrane electrode assembly (MEA) was obtained by pressing the cathode and anode on either side of a pretreated Nafion 115 membrane by compaction with a pressure of 50 kg/cm^2 at 135 °C for 3 min.

The DMFC was assembled by mounting the MEA into single cell with an active cross-sectional area of 4 cm^2. The single-cell test fixture has a dynamic hydrogen reference electrode (DHE); therefore, the cathode $I-V$ curve can be obtained. The single cell was "activated" by 1.0 M MeOH for 3 h at 90 °C, and then the cathode and the single-cell polarization curves were collected after the operation conditions of the single cell remained stable for half an hour. The operation conditions were the following: anode fuel, 1.0 M MeOH; flow rate, 1.0 mL/min; no backing pressure; oxygen pressure, 0.2 M Pa. All single-cell tests were conducted three times, and the results presented here are the average data.

Results and Discussion

It is well known that the multiwalled carbon nanotubes (MWNTs) prepared by the arc-discharge evaporation method are accompanied by many other forms of carbon particles. Therefore, it is necessary to use a strong oxidant to purify the raw MWNTs,[18,19] and then some surface modification procedures are applied to the purified MWNTs to have the Pt particles well deposited onto the MWNTs. Figure 1a shows that MWNTs

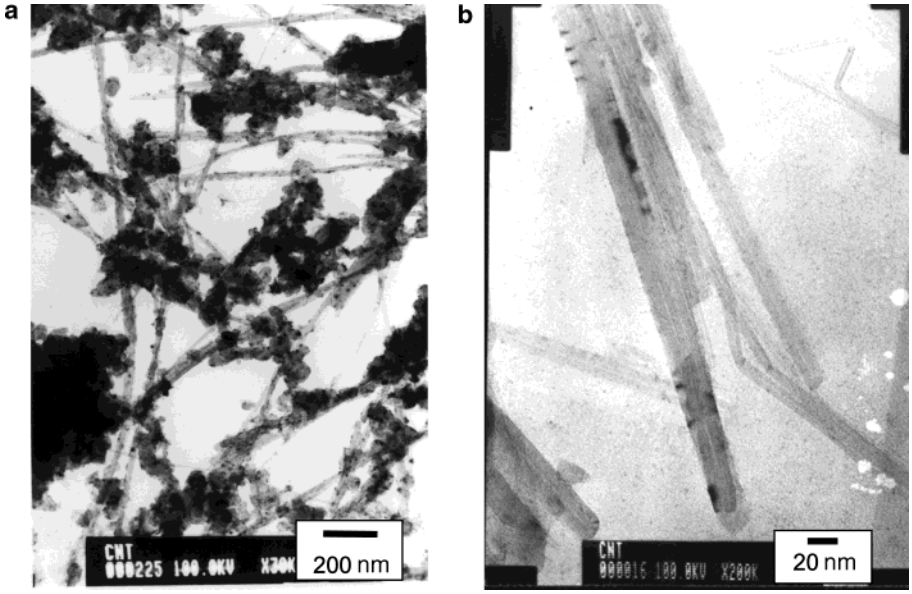

Figure 1. Bright-field TEM micrographs of (a) MWNTs without purification and (b) MWNTs after purification and $HNO_3-H_2SO_4$ oxidation.

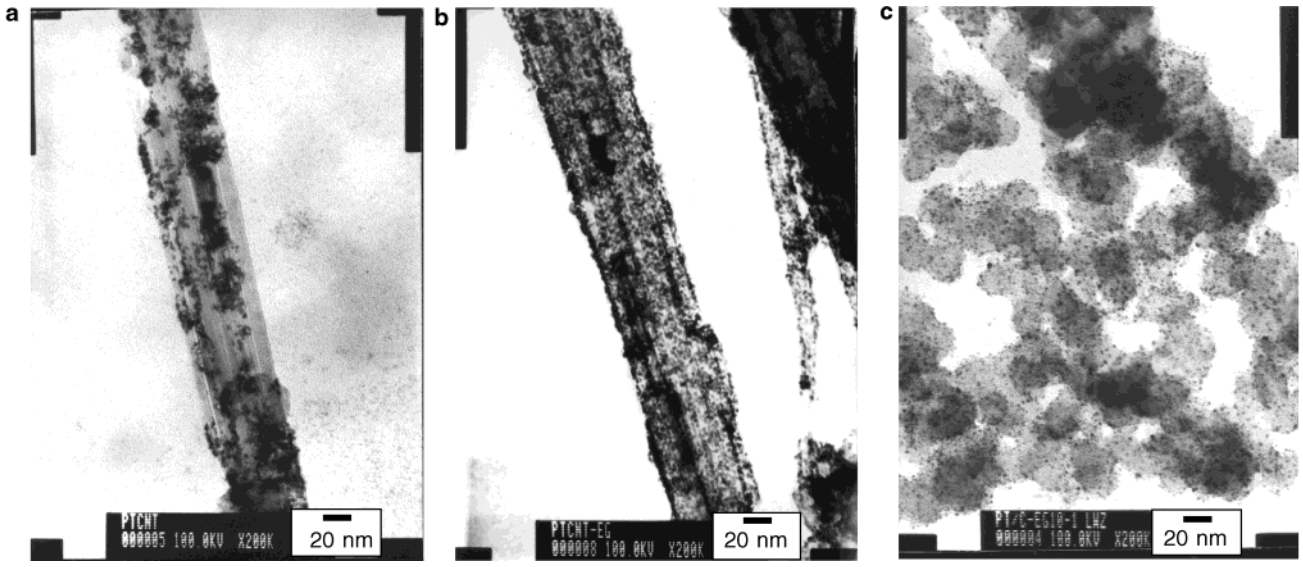

Figure 2. Bright-field TEM micrographs of (a) Pt/MWNT (A) (prepared by the HCHO method), (b) Pt/MWNT (B) (prepared by the EG method), and (c) Pt/XC-72 (prepared by the EG method) nanocomposites.

are stacked onto each other, accompanied by many carbon nanoparticles and many carbonaceous impurities. The MWNTs, after treatment by purification and slow oxidation in a mixture of $HNO_3-H_2SO_4$, are shown in Figure 1b, from which it can be seen that most MWNTs are isolated and nearly no carbon nanoparticle agglomeration is observed. The purification and oxidation pretreatment could result in a high density of surface functional groups on the raw MWNTs; among the functional groups are carboxyl, hydroxyl, and carbonyl groups.[26] The BET surface area of purified MWNTs is about 42 m^2/g, and this value increased about 20% (51 m^2/g) after surface oxidization treatment.

Figure 2a is the micrograph of Pt/MWNT (A) catalyst, which was reduced by HCHO in an aqueous solution. It can be seen from Figure 2a that Pt clusters agglomerate to some extent and disperse on the surface of MWNTs nonhomogeneously; Pt particles have a wide particle-size distribution ranging from 2 to 9 nm (Figure 3a) with a mean particle size of 3.4 nm. In contrast, in the Pt/MWNT (B) sample as shown in Figure 2b, a high and homogeneous dispersion of spherical Pt metal clusters is obtained. The histogram of Pt particle-size diameters for Pt/MWNT (B) shows that the Pt particles have a narrow size dispersion ranging from 2 to 5 nm with its peak centered at 2.6 nm, as can be seen in Figure 3b. Pt particles are located on both the inner and outer surfaces of the MWNTs. It appears that these MWNTs have similar diameters (Figure 2a and b); however, the distribution of Pt particle is very different. The dispersion of Pt particles may be correlated with the oxidation of MWNTs (i.e., more surface functional groups, caused by the oxidation of the MWNT surface, appear to result in a higher density of Pt particles). The oxidized MWNTs are more homogeneous in an EG solvent than in an aqueous solvent; maybe this factor also determines the Pt distribution on MWNTs because Pt precursors interact with MWNTs better in EG solvents, which results in more Pt deposition on the support. The HRTEM image in Figure 4 shows relatively small round particles with high contrast, as expected for crystalline metal nanoclusters, and the Pt particle size is about 3−4 nm. No specific Pt crystallinity was observed. In the case of XC-72 carbon (Figure 2c), a similar experiment results in the formation of a similar Pt particle distribution (2−4 nm) with particles having an average diameter of 2.2 nm. This implies that the

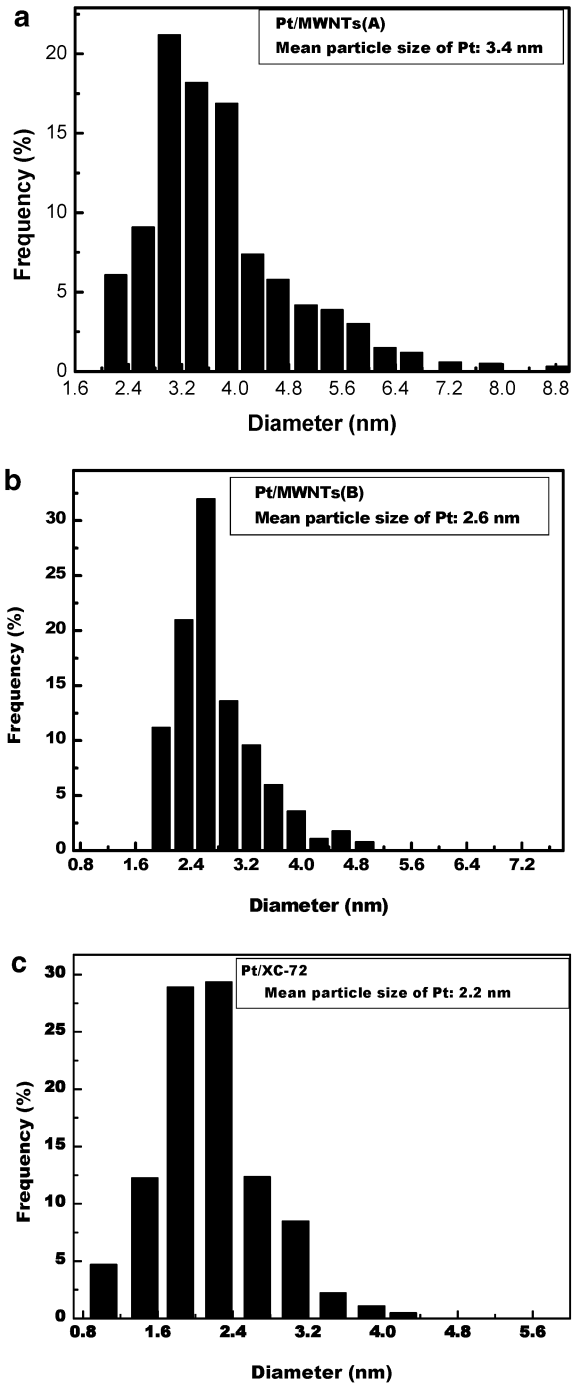

Figure 3. Histogram of Pt metal particle diameters for nanocomposites (a) Pt/MWNTs (A), (b) Pt/MWNTs (B), and (c) Pt/XC-72.

EG synthesis method could lead to the formation of homogeneous and small particles on different carbons (MWNTs or XC-72).

The XRD patterns of MWNTs and XC-72 carbon are shown in Figure 5. The diffraction peaks at 26.5°, 42.4°, 54.7°, and 77.4° observed in the diffraction of MWNTs can be attributed to the hexagonal graphite structures (002), (100), (004), and (110). For XC-72 carbon, a rather wide and shallow (002) peak is observed in its XRD pattern, implying that XC-72 is an amorphous carbon material with small regions of crystallinity and MWNTs are in graphite form. Figure 6a shows that Pt supported on both XC-72 and MWNT supports forms a face-centered cubic (fcc) structure and has major peaks at around $2\theta = 39.7°$ (111), 46.2° (200), 67.4° (220), and 81.2° (311). Because the Pt (220) peak is isolated from the carbon-support

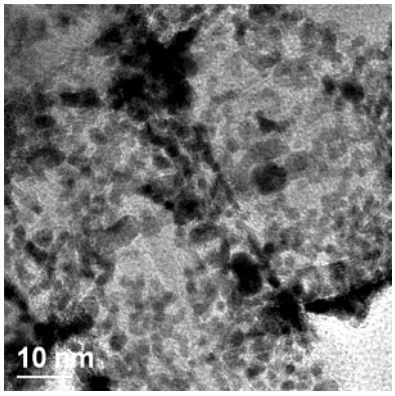

Figure 4. HRTEM micrograph of the Pt/MWNT (B) nanocomposite.

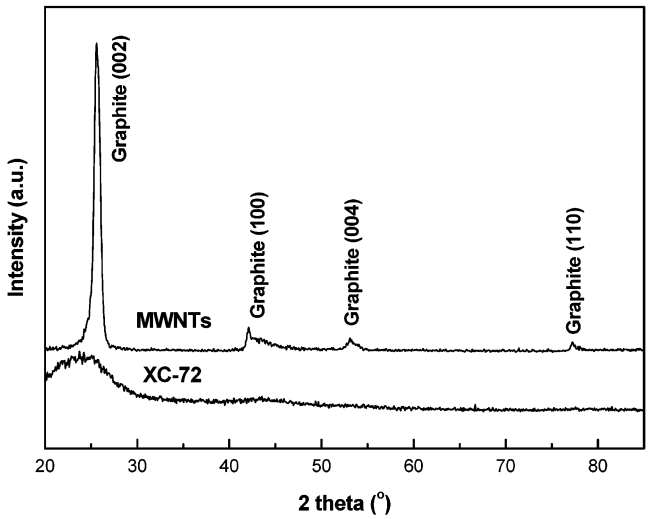

Figure 5. Powder X-ray diffraction patterns of MWNTs after purification and oxidation and XC-72 carbon black.

graphite diffraction peaks, the mean size of Pt particles can be calculated from this peak (Figure 6b) according to Scherrer's formula, [37] as shown below:

$$L = \frac{0.9\lambda_{K\alpha 1}}{B_{(2\theta)} \cos \theta_{max}}$$

L is the mean size of the Pt particles, $\lambda_{K\alpha 1}$ is the X-ray wavelength (Cu Kα $\lambda_{K\alpha 1} = 1.5418$ Å), θ_{max} is the maximum angle of the (220) peak, and $B_{(2\theta)}$ is the half-peak width for Pt (220) in radians. Thus, the mean particle sizes of these Pt-based catalysts are 2.1 nm for Pt/XC-72, 3.1 nm for Pt/MWNT (A), and 2.5 nm for Pt/MWNT (B), which are in good agreement with TEM results.

The preparation of chemically modified MWNT-deposited Pt nanocomposites was reported; however, Pt was reduced by hydrogen in aqueous solution, and the mean size of a Pt particle was about 10−20 nm.[26] Lordi and co-workers also used the ethylene glycol method to deposit Pt metal particles onto single-walled carbon nanotubes (SWNTs).[38] In the current study, it was found that the Pt particle size and distribution are not sensitive to the ratio of solvent to MWNTs. In our case, the Pt nanoparticles were deposited onto surface-oxidized MWNTs in a higher ratio of solvent to MWNTs, which is about 20 times higher than the ratio for the preparation of Pt/SWMTs reported in ref 38. The difference may be attributed to the different properties of the nanotube supports used and the different functional-group densities on the outer surface of MWNTs and SWNTs. In the case of the EG method, we found that the ratio

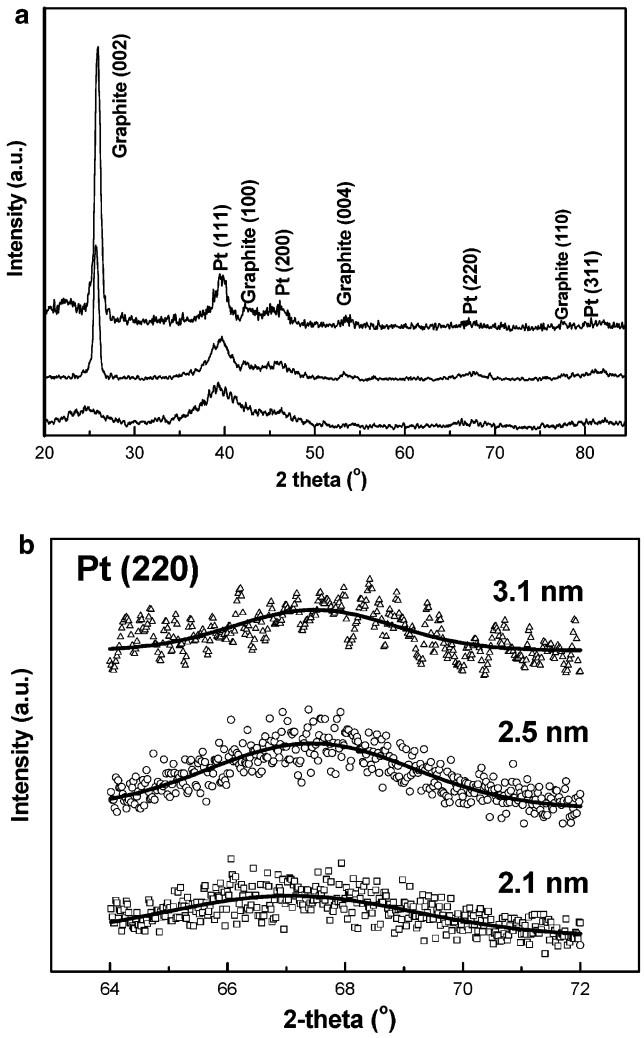

Figure 6. **(a)** Powder X-ray diffraction patterns of Pt/MWNTs (A), Pt/MWNTs (B), and Pt/XC-72 (from top to bottom). **(b)** Detailed Pt (220) peaks in the powder XRD patterns of Pt/MWNTs (A), Pt/MWNTs (B), and Pt/XC-72 (from top to bottom).

TABLE 1: Effect of DI Water Content in EG Solution on the Preparation of Pt/MWNTs[a]

DI water content (%, volume ratio)	Pt particle size (nm)
0	2.0
5	2.5
15	3.2
40	4.0
70	4.5

[a] Determined by the Scherrer formula from the Pt (220) peak.

of ethylene glycol solvent to DI water was one of the key factors in the particle size and distribution of Pt particles being deposited onto the MWNTs. As shown in Table 1, the mean size of the Pt particles is 2.0 nm when pure EG is the solvent, and the mean size of the Pt particles increases to about 4.0 nm when the water content is 40 vol %. In another words, smaller and more homogeneous Pt particles were obtained by increasing the concentration of EG. This means that the Pt particle size and distribution can be controlled, to some extent, by simply adjusting the water content. Wang et al. once reported a polyalcohol synthesis strategy for the preparation of unsupported noble-metal (Pt, Ru, Rh, etc.) nanoclusters with very small particle sizes and a very narrow particle distribution, in which they found that the metal particle size was very sensitive to the

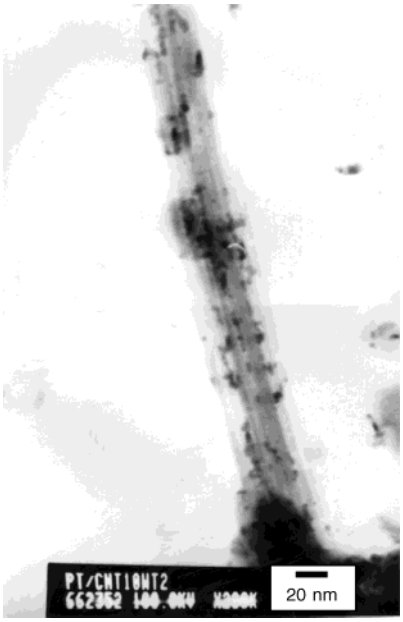

Figure 7. Bright-field TEM micrograph of Pt/MWNTs (MWNTs with purification but without surface oxidation, prepared by the EG method).

water content of the solvent; the size of the Pt particles that were obtained was about 1.1 nm when no water was added and about 2.4 nm when the water content was increased to 9 vol %.[39]

However, under the preparation conditions adopted in our study, in addition to water content, the surface modification of MWNTs is another important factor in the deposition of Pt particles. It is found that the Pt particles are deposited onto the nanotubes randomly and sparsely when MWNTs without surface oxidation are employed as supports (as can be seen in Figure 7). The detailed mechanism involved in the deposition process for the homogeneous dispersion of Pt in the Pt/MWNT (B) sample is not completely clear at the moment. Here we propose a scheme that would shed some light on the mechanism involved in the formation of nanosized Pt particles. The starting MWNT support materials used in our study are treated or slowly oxidized in a mixture of $HNO_3-H_2SO_4$, which would result in a high density of functional groups such as carboxyl, hydroxyl, and carbonyl group on MWNTs. After Pt precursors were added and mixed with surface-oxidized MWNTs, the Pt ions would interact with and attach to these surface functional groups on MWNTs via a coordination reaction or an ion-exchange reaction,[26] thus functioning as a nucleation precursor that is finally reduced by ethylene glycol to produce nanosized Pt particles. UV−vis, in situ NMR, and GC−MS analyses suggest that this reduction process may follow a one-step reaction to form glyoxal (CHO−CHO) when the redox reaction operates under similar conditions.[40] The whole preparation process would effectively control the particles size and distribution of Pt particles under the synthesis conditions at which the following two conditions are met: the nucleation step is quick and homogeneous, and at the same time, the nucleation and growth steps are completely separated. Furthermore, it can be expected that the growth of Pt particles would be restricted in a denser ethylene glycol solution than in an aqueous solvent, thus with decreasing concentration of EG, the particle size of Pt particles increases to a value that is even larger than that of Pt/MWNTs (A).

Cathodic polarizations obtained in direct methanol fuel cells (DMFCs) are presented in Figure 8a. Identical anode catalysts based on a 30 wt % Pt−Ru/C catalyst were used in all of the

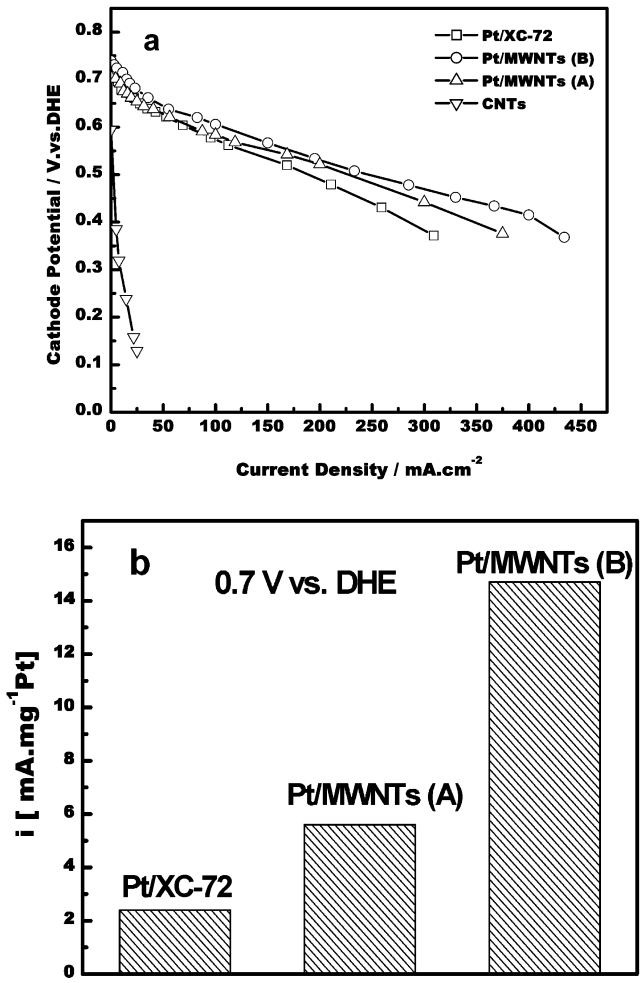

Figure 8. (a**)** Comparison of the cathode polarization curves for the oxygen reduction reaction in the DMFC at Pt/XC-72, Pt/MWNT (A, B), or MWNT cathode catalysts; anode: Pt−Ru/C (20 wt % Pt, 10 wt % Ru, Johnson Matthey Corp.; catalyst loading: 2.0 mg Pt−Ru/cm^2); electrolyte membrane: Nafion-115 (Dupont) membranes; operating temperature: 90 °C; methanol concentration: 1.0 M; flow rate: 1.0 mL/min; oxygen pressure: 0.2 MPa. (b**)** Comparison of the mass activity at 0.7 V obtained on Pt/XC-72, Pt/MWNT (A), and Pt/MWNT (B) catalysts.

experiments. Blank activity tests conducted on MWNT supports showed that it was not active in the ORR. The same Pt metal loading of these Pt-based catalysts for cathodes is employed (1.0 mgPt/cm^2). At a cathodic potential of 700 mV (vs DHE in the activation-controlled region), the current density of DMFC was 5.7 mA/mg Pt for Pt/MWNTs(A), 14.7 mA/mg Pt for Pt/MWNTs(B), and only 2.5 mA/mg Pt for Pt/XC-72 (as can be seen in Figure 8b), which means that the MWNT-supported platinum catalysts (A and B samples) show higher ORR mass activity in the activation-controlled region. Pt particles with a highly crystalline faceted structure that are dispersed on the highly tailored GNFs are relatively thin, thus they exhibit improved methanol oxidation activity that is 4 times higher than that of Vulcan XC-72 carbon.[29] However, Pt in the Pt/MWNT catalysts has globular morphology according to TEM images. HRTEM examination also shows that Pt particles are deposited on the outer walls of MWNTs, and no specific Pt crystals are observed. Therefore, the increased ORR activity of Pt/MWNTs may be attributed to the unique structure and good electrical properties of MWNTs, which would help to increase the electrical conductivity of MWNT supports when compared to that of a commercial Vulcan carbon XC-72 support. As we knew, MWNTs are made from high-purity graphite, and the electrical conductivity of graphite is much higher than that of XC-72 (graphite: 200−2500 S cm^{-1} (horizontal), 5.0 S cm^{-1} (vertical); XC-72: 4.0 S cm^{-1}).[41] Britto et al. studied the electrocatalysis of ORRs for MWNTs and graphite in H_2SO_4 electrolyte and found that the values of the exchange current density for MWNTs are at least 5 times higher than that for graphite. They also conducted ab initio density functional theory calculations on MWNTs and made use of the molecular dynamics (MD) simulation method to study the adsorptive dissociation of oxygen on MWNT surfaces and the charge-transfer process. They have demonstrated that the pentagons at the nanotube tips, the pentagon−heptagon defect pairs in the lattice, and the curvature are responsible for the improved behavior of the ORR.[16] The in situ resistivities of MEA with GNF-supported Pt catalysts were tested, and higher electrical conductivity for Pt/GNF nanocomposites was obtained.[30] In our case, we demonstrated the enhancement of the ORR for Pt/MWNT catalysts as compared to that of Pt/XC-72 in direct methanol fuel cell. In addition, the MWNT supports used in our study contain fewer organic impurities in comparison to the number in the commercial XC-72 carbon that used to contain 0.5 at % organosulfur impurities. Even after being treated with hydrochloric acid, the XC-72 carbon still contains sulfur (ca. 0.2 at. %), which poisons the Pt metal during common electrode pretreatmet.[29] However, no sulfur species were detected in the MWNT supports because the MWNTs were made from high-purity graphite and sulfate that was created and formed in the following surface-modification step was removed after reduction of Pt and filtration. Furthermore, we should not neglect another important factor—the pore structures of supports, which influence the reactant−product mass transport and therefore determine the activities of catalysts. XC-72 carbon has a BET surface area of 237 m^2/g with nearly 47% being micropores (<2 nm),[42,43] and these micropores do not make a contribution to the ORR, as can be expected. In the case of MWNTs whose diameter is in the range of 4−60 nm, of which most are greater than 10 nm and no micropores smaller than 2 nm are present, when MWNTs are employed as catalyst supports, the unique structure of the MWNTs should facilitate the water−oxygen mass transport that helps to improve the ORR property greatly. Similar results can be found in the literature[23] in which carbon nanofibers with a diameter of about 50 nm were used as a support for a Pd catalyst for the selective hydrogenation of the C=C bond in α,β-unsaturated cinnamaldehyde in the liquid phase, and it was found that the mass-transfer limitation in the hydrogenation reaction was improved significantly. The detailed mechanism of how the MWNTs would facilitate water−oxygen mass transport is not known at the moment, and more work is required to clarify this. For example, well-aligned or assembled MWNTs in the electrode will be tested to see whether the performance of the ORR would be further improved.

It can also be seen from Figure 8b that the mass activity of Pt/MWNTs (B) is higher than that of Pt/MWNTs (A) (14.7 mA/mg Pt vs 5.2 mA/mg Pt). Some literature reported the ORR on carbon black supports where a maximum in the catalyst mass activity is recorded at about a 3.0−5.0 nm Pt particle size (ca.12.5 A g^{-1} for Pt particles with an average size of 2.0 nm; ca.14.0 A g^{-1} for Pt particles with an average particle size of 3.0−5.0 nm at 0.9 V vs SHE (standard hydrogen electrode)).[44−46] The maximum value in mass activity for the oxygen reduction reaction versus the particle size of Pt is derived from a compromise between the specific activity and the surface area of Pt particles. The mean particle sizes of Pt for these two

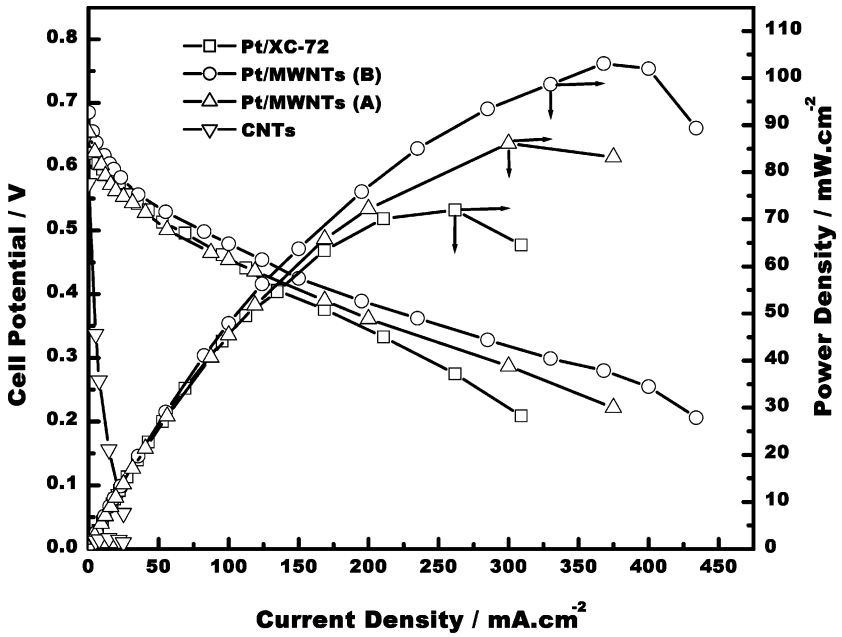

Figure 9. Comparison of single-cell polarization curves for the DMFC in the presence of Pt/XC-72, Pt/MWNT (A, B), or MWNT cathode catalysts; anode: Pt−Ru/C (20 wt % Pt, 10 wt % Ru, Johnson Matthey Corp.; catalyst loading: 2.0 mg Pt−Ru/cm^2); electrolyte membrane: Nafion-115 (Dupont) membranes; operation temperature: 90 °C; methanol concentration: 1.0 M; flow rate: 1.0 mL/min; oxygen pressure: 0.2 MPa.

MWNT-supported catalysts calculated from the XRD broadening (220) reflections are similar (3.1 nm (A) and 2.5 nm (B)). This suggests that another factor or parameter may be involved in influencing the ORR activity; that is, the different morphology and dispersion degree of Pt particles in the Pt/MWNT catalysts resulted from different preparation methods. TEM analysis shows a high and homogeneous platinum distribution in the Pt/MWNT (B) catalyst, which probably results in an enhanced interaction between Pt and MWNTs and thus leads to a higher mass activity.

Further enhancements in DMFC performance are observed in Figure 9 by using an MWNT cathode in comparison to an XC-72 cathode in the high current-density region. The current density at 0.4 V for the Pt/MWNT (B) catalyst is 186 mA/cm^2, which is 37% higher than the value of 136 mA/cm^2 for the Pt/XC-72 catalyst under the same test conditions. At a current density of 300 mA/cm^2, the Pt/MWNT (B) catalyst produces a cell potential that is 100 mV higher than that of the Pt/XC-72 catalyst. The limited current density and maximum power density of the single cell with Pt/MWNT (B) catalysts are 434 mA/cm^2 and 103 mW/cm^2, respectively; for the single cell with Pt/MWNT (A), the limited current density and maximum power density are 375 mA/cm^2 and 87 mW/cm^2, respectively, and in the case of DMFC with the Pt/XC-72 catalyst, the corresponding limited current density and maximum power density are only 309 mA/cm^2 and 70 mW/cm^2, respectively. The above results were obtained under the following identical conditions: The Pt metal loading of the cathode for all DMFCs was maintained at 1.0 mg/cm^2. The catalyst layer of DMFC with the Pt/MWNT cathode was about 30 μm, which is thinner than that of DMFCs with the Pt/XC-72 cathode (about 100 μm); therefore, better oxygen−water mass transport can be achieved in the catalyst layer. Higher metal loading Pt-based catalysts (60 wt %) were used to lower the catalytic layer in order to enhance mass transport.[47] Our results presented here show that by using MWNTs as supports this objective can be achieved with catalysts of lower platinum metal loading. Furthermore, the lower agglomeration degree of metal particles in the Pt/MWNT (B) catalyst would give the reactants easy access to the catalytic active sites, which would help to improve the mass transport in the cell system further.

Conclusions

This study presents two preparation methods for multiwalled carbon nanotube-supported platinum nanoparticle catalysts as cathode catalysts in DMFCs. The XRD, TEM, and HRTEM characterizations reveal that the high and homogeneous dispersion of Pt particles for the Pt/MWNTs can be prepared by the EG method. Surface modification of MWNTs and water content in EG solvent are found to be the key factors in controlling the particle size and distribution of Pt particles deposited on the MWNT support. All MWNT-supported Pt catalysts show enhanced ORR activities and superior cell performance in comparison to a XC-72-supported Pt catalyst. The high electrocatalytic activity may be attributed to the unique structural and higher electrical properties and the small number of organic impurities of MWNTs. The Pt/MWNT catalyst prepared by the EG method is superior to the catalyst prepared by the aqueous HCHO reduction method, suggesting that the different morphology and dispersion of Pt in MWNT-supported platinum catalysts also play an important role in the enhancement of ORR activity.

Acknowledgment. This work was partly supported by the National Natural Science Foundation of China (grant nos. 29976006 and 20173060), the Natural Science Foundation of the Liaoning Province of China (grant no. 9810300701), and the Foundation for University Key Teachers by the Education Ministry of China.

References and Notes

(1) Hamnett, A. *Catal. Today* **1997**, *38*, 445.
(2) McNicol, B. D.; Rand, D. A. J.; Williams, K. R. *J. Power Sources* **1999**, *83*, 15.
(3) Wasmus, S.; Kuver, A. *J. Electroanal. Chem.* **1999**, *461*, 14.
(4) Arico, A. S.; Srinivasan, S.; Antonucci, V. *Fuel Cells* **2001**, *2*, 1.
(5) Ren, X. M.; Zelenay, P.; Thomas, A.; Davey, J.; Gottesfeld, S. *J. Power Sources* **2000**, *86*, 111.
(6) Scott, K.; Taama, W. M.; Argyropoulos, P. *J. Power Sources* **1999**, *76*, 43.

(7) Shukla, A. K.; Neergat, M.; Parthasarathi, B.; Jayaram, V.; Hegde, M. S. *J. Electroanal. Chem*. **2001**, *504*, 111.
(8) Trapp, V.; Christensen, P. A.; Hamnett, A. *J. Chem. Soc., Faraday Trans.* **1996**, *21*, 4311.
(9) Reeve, R. W.; Christensen, P. A.; Hamnett, A.; Haydock, S. A.; Roy, S. C. *J. Electrochem. Soc*. **1998**, *145*, 3463.
(10) Tributsch, H.; Bron, M.; Hilgendorff, M.; Schulenburg, H.; Dorbant, I.; Eyert, V.; Bogdanoff, P.; Fiechter, S. *J. Appl. Electrochem.* **2001**, *31*, 739.
(11) Mukerjee, S.; Srinivasan, S.; Soriaga, M. P.; McBreen *J. Electrochem. Soc.* **1995**, *142*, 1409.
(12) Mukerjee, S.; Srinivasan, S. *J. Electroanal. Chem.* **1993**, *357*, 201.
(13) Capuano, G. A.; Thamizhmani, G. *J. Electrochem. Soc.* **1994**, *141*, 968.
(14) Arico, A. S.; Shukla, A. K.; Kim, H.; Park, S.; Min, M.; Antonucci, V. *Appl. Surf. Sci.* **2001**, *172*, 33.
(15) Neergat, M.; Shukla, A. K.; Gandhi, K. S. *J. Appl. Electrochem.* **2001**, *31*, 373.
(16) Britto, P. J.; Santhanam; K. S. V.; Rubio, A.; Alonso. J. A. A.; Ajayan, P. M.; *Adv. Mater*. **1999**, *11*, 154.
(17) Ravikumar, M. K.; Shukla, A. K. *J. Electrochem. Soc*. **1996**, *143*, 2601.
(18) Iijima, S. *Nature* **1991**, *354*, 56.
(19) Ebbesen, T. W.; Ajayan, P. M. *Nature* **1992**, *358*, 220.
(20) Li, W. Z.; Xie, S. S.; Qian, L. X.; Chang, B. H.; Zou, B. S.; Zhou, W. Y.; Zhao, R. A.; Wang, G. *Science* **1996**, *274*, 1701.
(21) Coq, B.; Planeix, J. M.; Brontons, V. *Appl. Catal*. **1998**, *173*, 175.
(22) Planeix, J. M.; Coustel, N.; Coq, B.; Brotons, V.; Kumbhar, P. S.; Dutartre, R.; Geneste, P.; Bernier, P.; Ajayan, P. M. *J. Am. Chem. Soc.* **1994**, *116*, 135.
(23) Pham, H. C.; Keller, N.; Charbonniere, L. J.; Ziessel, R.; Ledou, M. *Chem. Commun.* **2000**, 1871.
(24) Luo, J. Z.; Gao, L. Z.; Leong, Y. L.; Au, C. T. *Catal. Lett.* **2000**, *66*, 91.
(25) Liang, C. H.; Li, Z. L.; Qiu, J. S.; Li, C. *J. Catal.* **2002**, *211*, 278.
(26) Yu, R. Q.; Chen, L. W.; Liu, Q. P.; Lin, J. Y.; Tan, K. L.; Ng, S. C.; Chan, H.; Xu, G. Q.; Andyhor, T. S. *Chem. Mater*. **1998**, *10*, 718.
(27) Che, G. L.; Lakshmi, B. B.; Fisher, E. R.; Martin, C. R. *Nature* **1998**, *393*, 346.
(28) Joo, S. H.; Choi, S. J.; Oh, I.; Kwak, J.; Liu, Z.; Terasaki, O.; Ryoo, R. *Nature* **2001**, *412*, 169.
(29) Bessel, C. A.; Laubernds, K.; Rodriguez, N. M.; Baker, R. T. K. *J. Phys. Chem. B* **2001**, *105*, 1115.
(30) Steigerwalt, E. S.; Deluga, G. A.; Cliffel, D. E.; Lukehart, C. M. *J. Phys. Chem. B* **2001**, *105*, 8097.
(31) Boxall, D. L.; Deluga, G. A.; Kenik, E. A.; King, W. D.; Lukehart, C. M. *Chem. Mater*. **2001**, *13*, 891.
(32) Steigerwalt, E. S.; Deluga, G. A.; Lukehart, C. M. *J. Phys. Chem. B* **2002**, *106*, 760.
(33) Li, W. Z.; Liang, C. H.; Qiu, J. S.; Zhou, W. J.; Han, H. M.; Wei, Z. B.; Sun, G. Q.; Xin, Q. *Carbon* **2002**, *40*, 791.
(34) Askoylu, A. E.; Madalena, M.; Freitas; Figueiredo, J. L. *Appl. Catal., A* **2000**, *192*, 29.
(35) Xin, Q.; Li, W. Z.; Liang, C. H.; Zhou, Z. H.; Sun, G. Q. U.S. patent pending, 2002.
(36) Xin, Q.; Zhou, Z. H.; Zhou, W. J.; Li, W. Z.; Sun, G. Q Chinese Patent 01138909.5.
(37) Radmilovic, V.; Gasteiger, H. A.; Ross, P. N., Jr. *J. Catal.* **1995**, *154*, 98.
(38) Lordi, V.; Yao, N.; Wei, J. *Chem. Mater*. **2001**, *13*, 733−737.
(39) Wang, Y.; Ren, J. W.; Deng, K.; Gui, L. L.; Tang, Y. Q. *Chem. Mater*. **2000**, *12*, 1622.
(40) Zhou, Z. H.; Wang, S. L.; Zhou, W. J.; Wang, G. X.; Jiang, L. H.; Li, W. Z.; Song, S. Q.; Liu, J. G.; Sun, G. Q.; Xin, Q. *Chem. Commun.* **2003**, 394.
(41) Pantea, D.; Darmstadt, H.; Kaliaguine, S.; Summerchen, L.; Christian, R. *Carbon* **2001**, *39*, 1147−1158.
(42) Park, P. W.; Kwon, B. K.; Choi, J. H.; Park, I. S.; Kim, Y. M.; Sung, Y. E. *J. Power Sources* **2002**, *109*, 439.
(43) Uchida, M.; Aoyama, Y.; Tanabe, M.; Yanagihara, N.; Eda, N.; Ohta, A. *J. Electrochem. Soc*. **1995**, *142*, 8.
(44) Mukerjee, S. *J. Appl. Electrochem.* **1990**, *20*, 537.
(45) Kinoshita, K. *J. Electrochem. Soc*. **1990**, *137*, 845.
(46) Peuckert, M.; Yuneda, T.; Dalla Betta, R. A.; Boundart, M. *J. Electrochem. Soc*. **1986**, *113*, 944.
(47) Arico, A. S.; Creti, P.; Modica, E.; Monforte, G.; Baglio, V.; Antonnucci, V. *Electrochim. Acta* **2000**, *45*, 4319.